A time and ensemble equivalent linearization method for nonlinear systems under combined harmonic and random excitation

John Hickey[1,2] , Tore Butlin[2], Robin Langley[2] and Naoki Onozato[2,3]

Abstract

An Equivalent Linearization technique, termed an Equivalent Linearization Time and Ensemble Expectation (EL-TEE) approach, is used to develop an alternative method for estimating the response of a nonlinear oscillator to a combination of deterministic harmonic and random white noise excitation. The approach is based on applying equivalent linearization and averaging over the time period of one harmonic excitation cycle. This gives a set of coupled nonlinear equations that can be solved for the response averaged over time and across the ensemble. The primary advantages of the proposed method are its computational speed, ability to return physically meaningful linearization matrices and that it can be applied to a wide variety of nonlinearities. The method is applied to three example test systems: the well-known single degree of freedom Duffing oscillator; a single degree of freedom system with a displacement constraint imposing a discontinuous nonlinearity; and a multi degree of freedom oscillator with a localized polynomial nonlinearity that has also been examined experimentally. It is shown that the response predicted matches well with Monte Carlo results from direct time integration at a fraction of the computational cost, and the method is capable of reproducing key results observed experimentally.

Introduction

Many engineering vibration problems are approximated as systems that are either harmonically or randomly excited. However, in reality many dynamic systems are subjected to a combination of broadband noise and harmonic excitation, for example floating crane systems,[1] turbine blades under turbulent flows,[2] or energy harvesting devices.[3]

A variety of methods exist to predict vibration of structures under purely harmonic or random excitation. The commonly employed approaches are the harmonic balance method (HBM)[4] for harmonic inputs and equivalent linearization,[5,6] which is sometimes termed statistical linearization, for random excitation. Current practice for examining the dynamic behavior of nonlinear systems under combined excitation involves the use of time domain integration methods. However, this becomes prohibitively computationally expensive when Monte Carlo approaches are adopted to account for random loading. Therefore there is a need to develop new methods that can more efficiently predict the response of

nonlinear oscillators to combined harmonic and random loads.[7]

This problem has been explored by various researchers over the last 30 years. However, the literature in the field is rather disjointed, with many studies existing as standalone works without further development or wider application. Broadly speaking, the existing approaches to tackle the problem can be divided into two groups. The first group consists of methods based on combining nonlinear deterministic and stochastic dynamic analysis techniques to derive coupled equations which are then solved for the response quantities of interest. For example HBM has been used alongside Gaussian closure,[8,9]

[1]Department of Civil, Structural and Environmental Engineering, Trinity College Dublin, College Green, Dublin, Ireland
[2]Department of Engineering, University of Cambridge, Cambridge, UK
[3]Mitsubishi Heavy Industries Europe Ltd, Uxbridge, UK.

Corresponding author:
John Hickey, Department of Civil, Structural and Environmental Engineering, Trinity College Dublin, College Green, Dublin 2, Ireland.
Email: john.hickey@tcd.ie

stochastic averaging,[10] and equivalent linearization.[11] Spanos et al.[11] use HBM to derive a set of equations for the deterministic response component as functions of the random response statistical moments. Equivalent linearization, with the equivalent linear matrices averaged over a harmonic loading period, is then applied to the random response component, giving another set of equations involving the amplitudes of the harmonic response and the statistical moments of the random response. Combining these two sets of equations leads to a set of coupled nonlinear algebraic equations which can be solved for the two response components. As well as with HBM, equivalent linearization has also been applied in conjunction with both deterministic averaging[12] and stochastic averaging.[13,14] The method of multiple scales[15,16] is a perturbation analysis approach that has been employed extensively to study nonlinear oscillators.[17,18] Recently, a number of different studies have proposed alternative or modified perturbation methods, such as parameter splitting approaches[19,20] and the homotopy perturbation method,[21–23] that have shown improved performance for highly nonlinear oscillators under harmonic excitation. For combined excitation, the method of multiple scales has been employed in combination with Gaussian closure[24,25] deterministic averaging[26] and stochastic averaging,[27] or on its own in adapted forms for specific combined excitation problems.[28,29] The primary drawback of the majority of methods mentioned in the preceding section is that they can be difficult to generalize and have only been applied to highly specific and simple oscillators.

The second group of studies consists of Markovian methods that have been developed to examine the response probability density function. These works involve obtaining solutions to the Fokker-Planck Kolmogorv (FPK) equations, which are often, although not always, derived via stochastic averaging.[3,30–35] Exact analytical solutions for the FPK equations are available in a very limited number of cases,[36] however in general it is necessary to use more computationally expensive numerical techniques, such as cell mapping[37] or path integration.[38] The computational cost and complexity of implementation can make these approaches unattractive.

While there is clearly a reasonable amount of literature proposing methods to predict nonlinear response to combined excitation, many of the studies are specific to the particular nonlinearity under examination. For example, in Refs.[9,10,12,26,35] the methods are presented specifically for the Duffing oscillator, while Anh et al.[13] and Manohar and Iyengar[14] are specific to the van der Pol oscillator. This means that the proposed methods cannot be easily applied to alternative nonlinearities, particularly for nonlinearities that are not polynomial, like contact or friction nonlinearities. The need for methods with such

flexibility has recently been identified by Kong and Spanos, who have extended the method proposed by Spanos et al.[11] for application to systems with hysteretic nonlinearities.[39] Another limitation of the existing literature, also identified by identified by Spanos et al.,[11] is that many existing studies focus on single degree of freedom systems.

Considering these limitations, the fundamental aim of the work discussed in this paper is to develop a computationally efficient method to predict the response to combined excitation that can be readily applied to oscillators with a variety of nonlinearities and can be easily scaled to multi degree of freedom systems. The method proposed for this purpose is an equivalent linearization approach referred to as a Time and Ensemble Expectation (EL-TEE) method. The approach is based on defining a cost function that averages across the ensemble of random responses (as per equivalent linearization[6]) as well as taking the average over the time period of a harmonic loading cycle under "steady-state" conditions, that is, once the deterministic component of the starting transient has decayed. The formulation proposed in this paper is different to that in Spanos et al.[11] and Kong and Spanos,[39] as no distinction is made between the deterministic and random response components in the linearization. This allows the equations to be formulated in such a way that they return physically meaningful linearization matrices, that can provide further insight into system behavior. In contrast, the approach proposed in Spanos et al.[11] and Kong and Spanos,[39] separates the response into random and harmonic components before linearizing. This provides an extra degree of flexibility for the linearization, meaning in theory it is a more accurate approach. However, it does not return physically meaningful linearization matrices.

By linearizing over time and across the ensemble, a set of governing nonlinear equations is derived. These can be solved simultaneously to find the response averaged over time and across the ensemble. The proposed approach is applied to three example systems to demonstrate its applicability and versatility. Firstly a numerical model of a single degree of freedom oscillator with a cubic nonlinearity is examined, and the results are compared to those from both time integration and linearization method proposed in Spanos et al.[11] and Kong and Spanos.[39]1139 Once it is shown that the performance of the two linearization approaches is similar for this simple example, the method proposed here is applied for two more complex examples. Firstly for an oscillator with a discontinuous "end-stop" nonlinearity; and then to perform numerical simulation of an experimental test rig consisting of a multi degree of freedom beam with a localized nonlinear stiffness.

Derivation

Equivalent linearization – time and ensemble expectation (EL-TEE) method

The equation of motion describing the response of a nonlinear system with a velocity and displacement dependent nonlinearity can be written as:

$$\mathbf{M\ddot{v}} + \mathbf{C\dot{v}} + \mathbf{Kv} + \mathbf{f_{nl}(v, \ \dot{v})} = \mathbf{p} \tag{1}$$

where $\mathbf{M}$, $\mathbf{C}$, and $\mathbf{K}$ are the mass, damping, and stiffness matrices respectively, $\mathbf{f_{nl}(v, \ \dot{v})}$ is the nonlinear restoring force, $\mathbf{p}$ is the excitation and $\mathbf{v}$ is the displacement.

Equation (1) can be linearized using an equivalent linear system:

$$\mathbf{M\ddot{v}} + \mathbf{C\dot{v}} + \mathbf{Kv} + \mathbf{C^e\dot{v}} + \mathbf{K^ev} + \mathbf{\gamma} \ = \mathbf{p} \tag{2}$$

where $\mathbf{C^e}$ and $\mathbf{K^e}$ are equivalent linear damping and stiffness matrices respectively and $\mathbf{\gamma}$ is an offset term. The error in the linearization, $\mathbf{\epsilon}$, is defined as the difference between equation (1) and it's linearized counterpart. Thus for the linearization described by equation (2):

$$\mathbf{\epsilon} \equiv \mathbf{f_{nl}} - \mathbf{C^e\dot{v}} - \mathbf{K^ev} - \mathbf{\gamma} \tag{3}$$

The system is assumed to be excited by a stationary random force plus a deterministic harmonic force of period T and frequency Ω. To minimize the error in the linearization, a cost function is introduced. This cost function is defined as the mean over one excitation period of the deterministic excitation component (i.e. the time expectation) of the expected value (i.e. the ensemble expectation, denoted E[.]) of the sum of squares of the error.

$$\text{minimize}: \frac{1}{T}\int_0^T \mathrm{E}\left[\mathbf{\epsilon}^{\mathrm{T}}\mathbf{\epsilon}\right] \mathrm{d}t \tag{4}$$

which is equivalent to:

$$\text{minimize}: \frac{1}{\mathrm{T}}\int_0^{\mathrm{T}} \mathrm{E}\left[\epsilon_1^2 + \epsilon_2^2 + \ldots + \epsilon_n^2\right] dt \tag{5}$$

where ϵ_n is the nth element in the vector $\mathbf{\epsilon}$, defined by equation (3). As linearization is performed across the ensemble and over time, the proposed approach is described as a Time and Ensemble Expectation (EL-TEE) method. The minimization is performed with respect to each element of the equivalent stiffness matrix, equivalent damping matrix and the offset vector:

$$\int_0^T \frac{\partial}{\partial K_{i,j}^e} \mathrm{E}\left[\mathbf{\epsilon}^{\mathrm{T}}\mathbf{\epsilon}\right] dt = 0 \tag{6}$$

$$\int_0^T \frac{\partial}{\partial C_{i,j}^e} \mathrm{E}\left[\mathbf{\epsilon}^{\mathrm{T}}\mathbf{\epsilon}\right] dt = 0 \tag{7}$$

$$\int_0^T \frac{\partial}{\partial \gamma_i} \mathrm{E}\left[\mathbf{\epsilon}^{\mathrm{T}}\mathbf{\epsilon}\right] dt = 0 \tag{8}$$

where $K_{i,j}^e$ and $C_{i,j}^e$ are the (i,j) elements of the matrices $\mathbf{K^e}$ and $\mathbf{C^e}$ respectively and γ_i is the ith element of the vector $\mathbf{\gamma}$. This gives the following linearization equations:

$$\int_0^T \mathrm{E}\left[\mathbf{f_{nl}v}^{\mathrm{T}}\right] \mathrm{d}t = \mathbf{K^e}\int_0^T \mathrm{E}\left[\mathbf{vv}^{\mathrm{T}}\right] \mathrm{d}t + \mathbf{C^e}\int_0^T \mathrm{E}\left[\mathbf{\dot{v}v}^{\mathrm{T}}\right] \mathrm{d}t$$
$$+ \mathbf{\gamma}\int_0^T \mathrm{E}\left[\mathbf{v}^{\mathrm{T}}\right] \mathrm{d}t \tag{9}$$

$$\int_0^T \mathrm{E}\left[\mathbf{f_{nl}\dot{v}}^{\mathrm{T}}\right] \mathrm{d}t = \mathbf{K^e}\int_0^T \mathrm{E}\left[\mathbf{v\dot{v}}^{\mathrm{T}}\right] \mathrm{d}t + \mathbf{C^e}\int_0^T \mathrm{E}\left[\mathbf{\dot{v}\dot{v}}^{\mathrm{T}}\right] \mathrm{d}t$$
$$+ \mathbf{\gamma}\int_0^T \mathrm{E}\left[\mathbf{\dot{v}}^{\mathrm{T}}\right] \mathrm{d}t \tag{10}$$

$$\int_0^T \mathrm{E}[\mathbf{f_{nl}}] \mathrm{d}t = \mathbf{K^e}\int_0^T \mathrm{E}[\mathbf{v}] \mathrm{d}t + \mathbf{C^e}\int_0^T \mathrm{E}[\mathbf{\dot{v}}] \mathrm{d}t + \mathbf{\gamma} \tag{11}$$

These linearization expressions can be expressed as a single system of equations

$$\int_0^T \mathrm{E}\left[\mathbf{zf_{nl}^{T}}\right] \mathrm{d}t = \int_0^T \mathrm{E}\left[\mathbf{zz}^{\mathrm{T}}\right] \mathrm{d}t \begin{bmatrix} \mathbf{K^{eT}} \\ \mathbf{C^{eT}} \\ \mathbf{\gamma}^{\mathrm{T}} \end{bmatrix} \tag{12}$$

where $\mathbf{z}$ is the vector:

$$z = \begin{Bmatrix} \mathbf{v} \\ \mathbf{\dot{v}} \\ 1 \end{Bmatrix} \tag{13}$$

The linearization matrices obtained by solving equation (12) can then be applied in equation (2) to calculate the response of the equivalent linear system. This is done by assuming that the response is stable such

that both the response and excitation can be separated into harmonic, zero-mean random and constant components, termed $\mathbf{v_h}$, $\mathbf{v_r}$, and $\bar{\mathbf{v}}$ and $\mathbf{p_h}$, $\mathbf{p_r}$, and $\bar{\mathbf{p}}$ respectively:

$$\mathbf{v} = \mathbf{v_h} + \mathbf{v_r} + \bar{\mathbf{v}} \tag{14}$$

$$\mathbf{p} = \mathbf{p_h} + \mathbf{p_r} + \bar{\mathbf{p}} \tag{15}$$

Using equations (14) and (15), equation (2) can be rewritten as:

$$\begin{aligned} \mathbf{M}(\ddot{\mathbf{v}}_\mathbf{h} + \ddot{\mathbf{v}}_\mathbf{r}) &+ (\mathbf{C} + \mathbf{C^e})(\dot{\mathbf{v}}_\mathbf{h} + \dot{\mathbf{v}}_\mathbf{r}) \\ &+ (\mathbf{K} + \mathbf{K^e})(\mathbf{v_h} + \mathbf{v_r} + \bar{\mathbf{v}}) + \boldsymbol{\gamma} = \mathbf{p_h} + \mathbf{p_r} + \bar{\mathbf{p}} \end{aligned} \tag{16}$$

Taking expectations across the ensemble and then separating the time independent and time varying terms gives two equations:

$$\mathbf{M}\ddot{\mathbf{v}}_\mathbf{h} + (\mathbf{C} + \mathbf{C^e})\dot{\mathbf{v}}_\mathbf{h} + (\mathbf{K} + \mathbf{K^e})\mathbf{v_h} = \mathbf{p_h} \tag{17}$$

$$(\mathbf{K} + \mathbf{K^e})\bar{\mathbf{v}} + \boldsymbol{\gamma} = \bar{\mathbf{p}} \tag{18}$$

Equation (17) can be solved using the standard steady-state solution for a harmonically driven oscillator with $\mathbf{p_h} = \mathbf{P_h}e^{i\Omega t}$ and $\mathbf{v_h} = \mathbf{V_h}e^{i\Omega t}$ (implicitly taking the real part):

$$\mathbf{v_h}(i\Omega) = \left[-\Omega^2\mathbf{M} + i\Omega(\mathbf{C} + \mathbf{C^e}) + (\mathbf{K} + \mathbf{K^e}) \right]^{-1}\mathbf{P_h} \tag{19}$$

where $\mathbf{P_h}$ and $\mathbf{V_h}$ are the complex amplitudes of the harmonic excitation and response respectively. Subtracting equations (17) and (18) from equation (16) leaves the equation governing the random response component:

$$\mathbf{M}\ddot{\mathbf{v}}_\mathbf{r} + (\mathbf{C} + \mathbf{C^e})\dot{\mathbf{v}}_\mathbf{r} + (\mathbf{K} + \mathbf{K^e})\mathbf{v_r} = \mathbf{p_r} \tag{20}$$

Standard frequency-domain linear random vibration theory can be used to solve equation (20) and obtain the cross-spectral density matrix of the random response component. The covariance matrix of the response can then be obtained by integrating each element of this across all frequencies. Alternatively, if it is assumed that the random excitation is Gaussian white noise with a spectral density matrix $\mathbf{S_0}$, the covariance matrix of the random response component can be obtained directly by solving the Lyapunov Equation describing the response of a randomly loaded oscillator[5]:

$$\mathbf{AV^T} + \mathbf{VA^T} = -\mathbf{G} \tag{21}$$

where:

$$A = \begin{bmatrix} \mathbf{0} & \mathbf{I} \\ -(\mathbf{K} + \mathbf{K^e}) & -(\mathbf{C} + \mathbf{C^e}) \end{bmatrix} \tag{22}$$

where $\mathbf{I}$ is the identity matrix. $\mathbf{V}$ is the covariance matrix of the random response component:

$$V = \begin{bmatrix} \mathrm{E}[\mathbf{v_r v_r}^T] & \mathrm{E}[\mathbf{v_r \dot{v}_r}^T] \\ \mathrm{E}[\dot{\mathbf{v}}_\mathbf{r}\mathbf{v_r}^T] & \mathrm{E}[\dot{\mathbf{v}}_\mathbf{r}\dot{\mathbf{v}}_\mathbf{r}^T] \end{bmatrix} \tag{23}$$

and $\mathbf{G}$ is given by

$$G = \begin{bmatrix} \mathbf{0} & \mathbf{0} \\ \mathbf{0} & 2\pi\mathbf{S_0} \end{bmatrix} \tag{24}$$

This Lyapunov Equation approach avoids the need for integration over frequency, thus improving computational efficiency compared to the more generally applicable spectral approach. Combining equations (12), (18), (19), and (21) allows the response of the system to be calculated by solving the nonlinear simultaneous equations:

$$\begin{bmatrix} \mathrm{E}[\mathbf{v_r v_r}] & \mathrm{E}[\mathbf{v_r \dot{v}_r}] \\ \mathrm{E}[\dot{\mathbf{v}}_\mathbf{r}\mathbf{v_r}] & \mathrm{E}[\dot{\mathbf{v}}_\mathbf{r}\dot{\mathbf{v}}_\mathbf{r}] \end{bmatrix} = \mathrm{Lyapunov}(\mathbf{A}, \mathbf{G}) \tag{25a}$$

$$\mathbf{V_h}(i\Omega) = \left[-\Omega^2\mathbf{M} + i\Omega(\mathbf{C} + \mathbf{C^e}) + (\mathbf{K} + \mathbf{K^e}) \right]^{-1}\mathbf{P_h} \tag{25b}$$

$$\bar{\mathbf{v}} = \left[(\mathbf{K} + \mathbf{K^e})\right]^{-1}\{\bar{\mathbf{p}} - \boldsymbol{\gamma}\} \tag{25c}$$

$$\int_0^T \mathrm{E}\left[\mathbf{z}\mathbf{f_{nl}^T}\right]\mathrm{d}t = \int_0^T \mathrm{E}\left[\mathbf{z}\mathbf{z^T}\right]\mathrm{d}t \begin{bmatrix} \mathbf{K^e}^T \\ \mathbf{C^e}^T \\ \boldsymbol{\gamma}^T \end{bmatrix} \tag{25d}$$

The Lyapunov Equation can be solved easily using standard solvers, for example the inbuilt `Lyap` function in `Matlab`. The system of equations in equation (25) can be solved using nonlinear solvers, such as the `fsolve` function in `Matlab`. Furthermore, when evaluating the expectations in equation 25(d), it can be assumed that the random response component $\mathbf{v_r}$ follows a Gaussian distribution. It should be noted that a general limitation of the equivalent linearization technique is that when applied to systems with Gaussian inputs the true, non-Gaussian, response distribution is approximated by a Gaussian distribution.

The root mean square value of the combined dynamic displacement once the deterministic component of the starting transient has decayed for degree of freedom p can be shown to be:

$$v_{rms,p} = \sqrt{\frac{V_{h,p}^2}{2} + \mathrm{E}[v_{r,p}v_{r,p}]} \tag{26}$$

where $V_{h,p}$ is the amplitude a of the harmonic displacement component of the response, $\mathbf{V}(i\Omega)$, at degree of freedom p and $E[y_{r,p}y_{r,p}]$ is the (p, p) element of the covariance matrix of random response $E[\mathbf{v_r v_r^T}]$. The dynamic response will be offset by the constant displacement component $\bar{v}_p$.

It is worth highlighting that in equivalent linearization of systems subjected to stationary excitation, it is common to represent the equivalent stiffness and damping matrices as the expected value of tangent matrices[5] such that:

$$\mathbf{K^e} = E\left[\frac{\partial \mathbf{f}}{\partial \mathbf{v}}\right] \tag{27}$$

$$\mathbf{C^e} = E\left[\frac{\partial \mathbf{f}}{\partial \dot{\mathbf{v}}}\right] \tag{28}$$

These expressions are derived from the fact that for a zero mean Gaussian random variable $\mathbf{y}$, it can be shown that[40]:

$$E[\mathbf{yf^T}] = E[\mathbf{yy^T}] E\left[\frac{\partial \mathbf{f}}{\partial \mathbf{y}}\right] \tag{29}$$

However, for the combined excitation problem under examination in this study, the response is not stationary, and the mean value changes over time with the harmonic response. If, as before, the response is assumed to consist of a zero mean random component, a harmonic component and a constant offset value, the expectation $E[\mathbf{zf_{nl}^T}]$ in equation (25d) can be expanded as:

$$E[\mathbf{zf_{nl}^T}] = E[\mathbf{z_h f_{nl}^T}] + E[\mathbf{z_r f_{nl}^T}] + E[\bar{\mathbf{z}}\mathbf{f_{nl}^T}] \tag{30}$$

Equation (29) can then be employed for the stationary zero-mean component, $E[\mathbf{z_r f_{nl}^T}]$, such that:

$$E[\mathbf{zf_{nl}^T}] = E[\mathbf{z_h f_{nl}^T}] + E[\mathbf{z_r z_r^T}] E\left[\frac{\partial \mathbf{f_{nl}^T}}{\partial \mathbf{z_r}}\right] + E[\bar{\mathbf{z}}\mathbf{f_{nl}^T}] \tag{31}$$

Therefore, while the "tangent matrix" simplification may be useful algebraically, for the linearization performed here it does not describe the complete solution as it does for zero mean stationary problems.

Finally, it is also necessary to point out how the derivation presented above differs from that proposed by Spanos et al.,[11,39] which for simplicity is termed the "Spanos Method" in this paper. The linearization presented in equation (2) makes no distinction between the random and deterministic response components; this is only introduced in equation (14) after the linearization matrices are derived. In contrast, in the Spanos Method, these two response components are treated separately. First order HBM is performed to examine the harmonic response, with the expected value of the nonlinear force represented using a Fourier expansion. Equivalent linearization averaged over a harmonic loading period is then performed to examine the random response component. This leads to a set of coupled equations. Separating the harmonic and random components relaxes the constraint of having a single linearized system and therefore in principle the Spanos Method can return a smaller error than the approach proposed in this paper. However, as the random and harmonic responses are treated separately, the linearization matrices obtained for Equivalent Linearization are the "tangent matrices" and essentially correspond to the second term in equation (31). This means these matrices do not have a physical meaning as they do not consider the impact of harmonic response, that is, they don't include the first or third term in equation (31). This contrasts with the approach proposed here, where no distinction is made between response components and physically meaningful linearized natural frequencies and damping rations are obtained. These can give further insight into the response of the system. The differences between the two approaches are demonstrated through application to a single degree of freedom (SDOF) Duffing oscillator in the following section.

Application to a SDOF Duffing oscillator

To practically apply the EL-TEE approach presented in Section 2, the expressions involving the function f_{nl}, which describes the nonlinearity, need to be evaluated. To demonstrate the versatility of the method, this is carried out here for three example systems, the first of which is the widely studied SDOF Duffing oscillator with a cubic nonlinearity. The nonlinear restoring force is given by:

$$f_{nl} = \lambda v^3 \tag{32}$$

To apply the EL-TEE approach to the Duffing oscillator, it is necessary to evaluate the linearization coefficients in equation (25) specifically for this nonlinearity. Firstly, it can be shown that $E[f\dot{v}] = 0$. This is as expected given that the nonlinearity is independent of velocity and there is no additional damping or energy dissipation, hence $C^e = 0$. The equivalent linear stiffness is given by equation (25d) and for a SDOF systems requires the evaluation of the integrals $\int_0^T E[f_{nl}v]dt$ and $\int_0^T E[v^2]dt$ using the nonlinearity defined by equation (32). In Appendix A this is shown to be:

$$K^e = \frac{\lambda \left(\frac{3}{8} V_h^4 + 3\left(E\left[v_r^2\right]\right)^2 + 3 V_h^2 E\left[v_r^2\right] \right)}{E\left[v_r^2\right] + \frac{1}{2} V_h^2} \qquad (33)$$

where P_h and V_h are the amplitudes of the harmonic excitation and response respectively. In the derivation of this expression it is assumed that the random response component follows a Gaussian distribution. Therefore, the linearization for a Duffing oscillator is defined by the coupled nonlinear simultaneous Equations:

$$E\left[v_r^2\right] = \frac{\pi S_0}{2\zeta\omega_n M(K + K^e)} \qquad (34a)$$

$$V_h(i\Omega) = \frac{P_h}{-\Omega M + i\Omega C + (K + K^e)} \qquad (34b)$$

$$K^e = \frac{\lambda \left(\frac{3}{8} V_h^4 + 3\left(E\left[v_r^2\right]\right)^2 + 3 V_h^2 E\left[v_r^2\right] \right)}{E\left[v_r^2\right] + \frac{1}{2} V_h^2} \qquad (34c)$$

It is useful to examine equation (34) in the three limiting cases of no nonlinear force ($\lambda = 0$), purely random excitation ($P_h = 0$) and purely harmonic excitation ($S_0 = 0$). Firstly, when $\lambda = 0$, the nonlinear stiffness K^e is equal to zero and the system of equations reduces to two uncoupled expressions describing the response of a linear system, as expected.

Secondly, for purely random excitation, that is, $P_h = 0$, equation (34b) leads to $V_h = 0$. In turn, this leads to $K^e = 3\lambda E\left[v_r^2\right]$. This is the same as the solution obtained from Equivalent Linearization for a Duffing oscillator subjected to random excitation.[5]

Finally, for purely harmonic excitation, where $S_0 = 0$, equation (34a) gives $E\left[v_r^2\right] = 0$. Thus, equation (34) reduces to:

$$v_h(i\Omega) = \frac{P_h}{[-\Omega M + i\Omega C + (K + K^e)]} \qquad (35a)$$

$$K^e = \frac{3}{4}\lambda V_h^2 \qquad (35b)$$

Equation (35a) is the standard equation for obtaining the amplitude of harmonic response for a system with stiffness $(K + K^e)$. Equation (35b) describes the value for the effective stiffness of a Duffing oscillator when linearized over one load cycle, and is the same as the effective stiffness derived using the first order HBM.[41] Another point of interest for this limiting case of purely harmonic excitation relates to the challenge of obtaining converged solutions across a range of excitation frequencies, particularly when the nonlinearity leads to jump-like behavior. This issue is discussed in the following section.

Example application to harmonic excitation & solution scheme

Figure 1(a) to (c) compare the steady-state RMS displacement response obtained from the EL-TEE method defined by equation (25) for purely harmonic excitation with the results of Time Integration. This is shown for three oscillators; a linear system where $\lambda = 0$, a system with a softening nonlinearity where $\lambda = -0.003$ and a hardening nonlinearity where $\lambda = 0.04$. All oscillators are assigned unit mass and stiffness (leading to unit circular frequency, i.e. $\omega_n = 1$) and a damping ratio of 5% (i.e. $\zeta = 0.05$). This choice of parameters is illustrative, leading to backbone curves that include jump phenomena but which do not exhibit chaotic behavior under harmonic excitation.

In Figure 1(a) to (c) the RMS displacement is shown as a function of normalized excitation frequency Ω/ω_n, with the hollow circles showing the results of time integration and the stars showing the results obtained from the proposed equivalent linearization approach. The proposed EL-TEE method matches well with the results of time integration. The EL-TEE approach does not consider initial conditions and therefore returns the two possible solutions in the unstable region, where the response is dependent on initial conditions. This contrasts with time integration, which considers a single scenario with specified initial conditions (at rest for the example in Figure 1) and which therefore only returns one solution for each harmonic excitation frequency. Consequently, there is a clearly defined jump between the two solution branches for time integration, whereas the proposed simply identifies the two possible solutions. In this sense, the output of the proposed method is similar to the results obtained from the first order HBM, albeit without the third (unstable) intermediate solution that can be obtained from that method. This is demonstrated in Figure 1(d), which shows the same case as Figure 1(c) but using HBM and including the unstable part of the solution.

The nonlinear equations of equation (34) are solved using the `fsolve` function in `Matlab`, which employs an iterative Newton Raphson scheme. To begin iteration a good initial guess for the solution is required. Therefore, for each change of excitation frequency, the solution for the previous excitation frequency is used as the initial guess. In order to generate the equivalent linearization results shown in Figure 1, the calculation is carried out by initially moving from "left to right" on the frequency axis, that is, increasing the frequency of harmonic excitation, until convergence fails, at which point the calculation is carried out "right-to-left," that is, decreasing the frequency of harmonic excitation.

This "left-to-right right-to-left" approach is the reason two possible solutions are found for frequencies in the unstable region for the nonlinear cases.
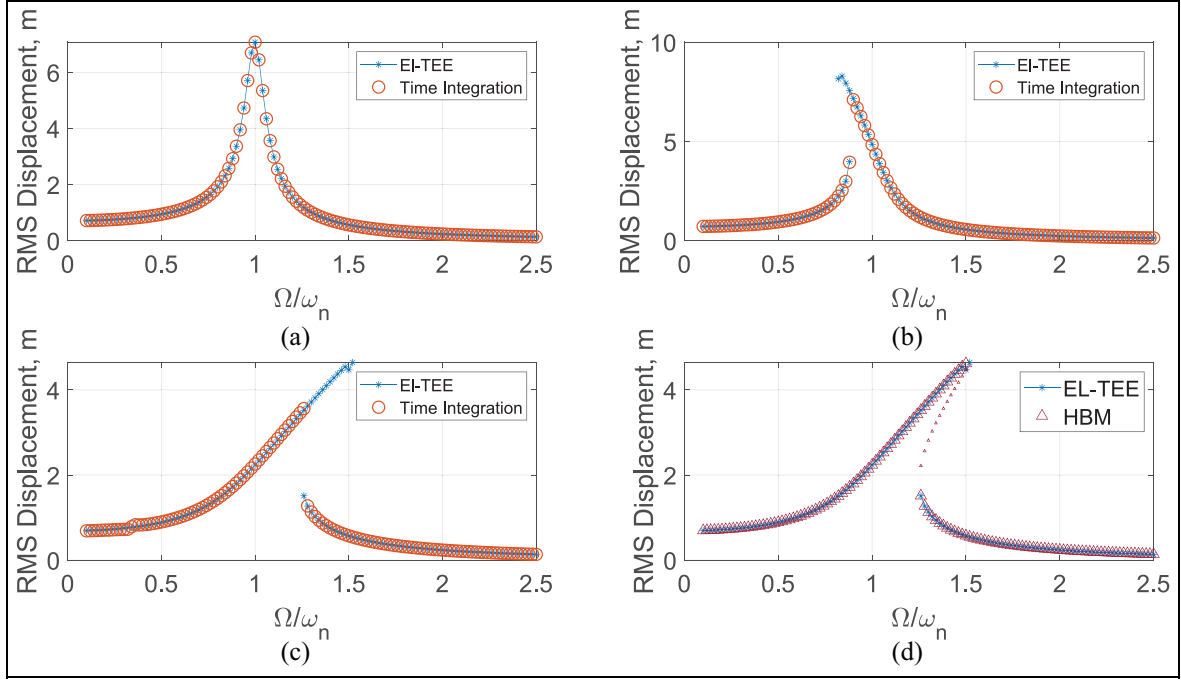
Figure 1. Comparison between results from EL-TEE and time integration for a Duffing oscillator subjected to harmonic excitation: (a) linear system $\lambda = 0$, (b) softening nonlinearity $\lambda = -0.003$, (c) hardening nonlinearity $\lambda = 0.04$. Comparison with results from HBM (d) hardening nonlinearity $\lambda = 0.04$.

More advanced continuation methods (e.g. Von Groll and Ewins [42]) have the potential to improve the convergence performance, but that is beyond the scope of the present investigation.

Quantifying the relative strength of random and harmonic loading components

For cases of combined excitation there is no obvious way to directly compare the strength of Gaussian white noise and harmonic excitation. This is because in the time domain, the root means square (RMS) value of white noise is theoretically infinite, while in the frequency domain the spectral amplitude of harmonic excitation is theoretically infinite. Therefore, it is proposed to compare the two excitation components via the resulting response of a linear oscillator. The root mean square (RMS) response of a harmonically driven single degree of freedom oscillator at the resonant frequency can be shown to be:

$$V_{h,\,rms} = \frac{P_h}{2\sqrt{2}\zeta M \omega_n^2} \tag{36}$$

where P_h is the amplitude of the harmonic excitation, ζ is the damping ratio and ω_n is the natural frequency of the system. The RMS response to random white noise excitation is given by:

$$v_{r,\,rms} = \sqrt{\frac{\pi S_0}{2\zeta M^2 \omega_n^3}} \tag{37}$$

Where S_0 is the constant value of spectral density measured in $N^2/(rad/s)$. A new term, α_{resp}, is defined as:

$$\alpha_{resp} \equiv \frac{v_{r,\,RMS}}{V_{h,\,RMS}} \tag{38}$$

Meaning that:

$$\alpha_{resp} = \frac{2\sqrt{\pi S_0 \zeta \omega_n}}{P_h} \tag{39}$$

Therefore α_{resp} is the dimensionless ratio of the response of a linear oscillator to Gaussian excitation to the response to harmonic excitation at the natural frequency. This provides a metric to quantify the relative strength of the two excitation components applied to a specific oscillator. However, as it depends on the viscous damping ratio and natural frequency, values for oscillators with different properties are not consistent and cannot be directly compared, in other words applying the same combined excitation to different oscillators results in a different α_{resp} value. This issue van be overcome if the constants, 2, π, and ζ, are removed from equation (39) (implicitly choosing
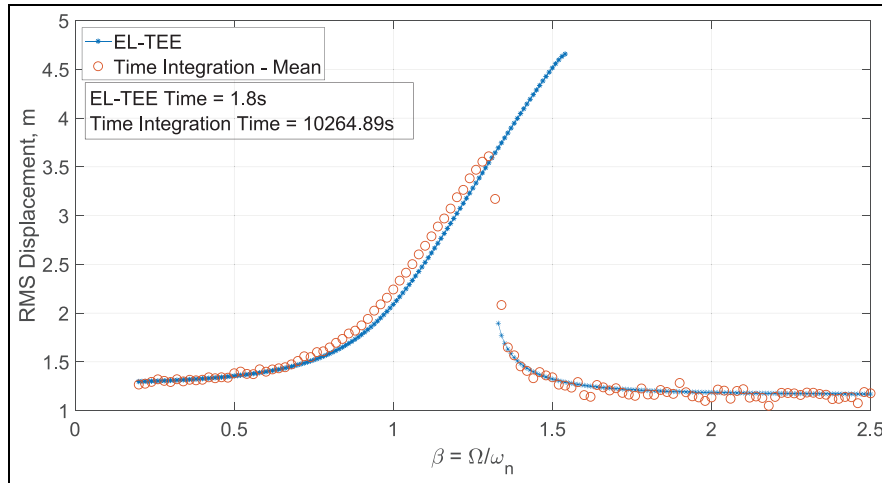
Figure 2. Comparison of the response of Duffing oscillator with hardening nonlinearity ($\lambda = 0.04$) to combined harmonic and random excitation ($\alpha = 0.32$) calculated using time integration and the proposed Time-and- Ensemble Expectation Equivalent Linearization (EL-TEE) method.

$\zeta = 1/4\pi$). This means it need not explicitly represent the ratio between the response of a linear oscillator to the two excitation components. The numerator now becomes the RMS of the random load, if the white noise is band limited to between 0 and the natural frequency ω_n. Likewise, dividing the denominator by $\sqrt{2}$ gives the RMS of the harmonic excitation component. Therefore, a separate, more versatile, parameter α, can be defined as the ratio between the RMS values of the random excitation component (with a cut off frequency ω_n) and the harmonic excitation component:

$$\alpha = \frac{\sqrt{2S_0\omega_n}}{P} \qquad (40)$$

This term is employed throughout this paper to quantify the applied combined excitations.

Application to combined excitation

Figure 2 and Supplemental Figure 1 show the effect of harmonic excitation frequency, Ω, on the steady-state RMS displacement response for Duffing oscillators with hardening ($\lambda = 0.04$) and softening ($\lambda = -0.003$) nonlinearity respectively. As in the previous section, both oscillators are assigned unit mass and stiffness and a damping ratio of 5% (i.e. $\omega_n = 1$, $\zeta = 0.05$). The oscillators are subjected to combined unit amplitude harmonic excitation and white noise excitation with constant spectral density of $S_0 = 0.05 \, \text{N}^2/(\text{rad/s})$. This corresponds to an α value of 0.32, as defined by equation (40). To provide benchmark results for comparison, a set of Monte Carlo time-domain simulations is carried out using 30 different random load time histories at each harmonic excitation frequency. The steady-state RMS displacement for each Monte Carlo realization

is estimated over 50 harmonic excitation periods once the deterministic component of the starting transient has decayed.

Results from time integration (hollow circles) are compared with the proposed EL-TEE method (stars). Firstly, over most of the range of excitation frequencies for both the hardening and softening case these RMS values obtained from the proposed equivalent linearization method are similar to the mean values obtained from the Monte Carlo time integration, showing that the method works well. Secondly, the computation times for both approaches are also presented in the Figure 2 and Supplemental Figure 1; where the equivalent linearization approach is approximately four orders of magnitude faster than the Monte Carlo time integration employed.

As in the case of harmonic excitation discussed previously, the equivalent linearization solution returns two solution branches which, for the hardening nonlinearity, results in a region where the upper branch is not seen in the time integration simulations. Figure 2 also shows that for frequencies near the jump phenomena ($\beta \approx 1.3$) the time integration results show intermediate values, giving a smoother transition than the sudden jump seen in Figure 1(c). This is because the jump frequency is not deterministic in the presence of a random loading component. For purely harmonic excitation, the jump occurs at a clearly defined frequency. However, in the presence of random excitation this jump can occur over a range of frequencies, meaning that near the jump frequency the RMS response for some realizations corresponds to the upper branch and some to the lower branch. Thus, the average value lies between the two stable solutions.

In terms of computational time the proposed EL-TEE method is substantially faster than Monte Carlo time domain integration. For example, in the
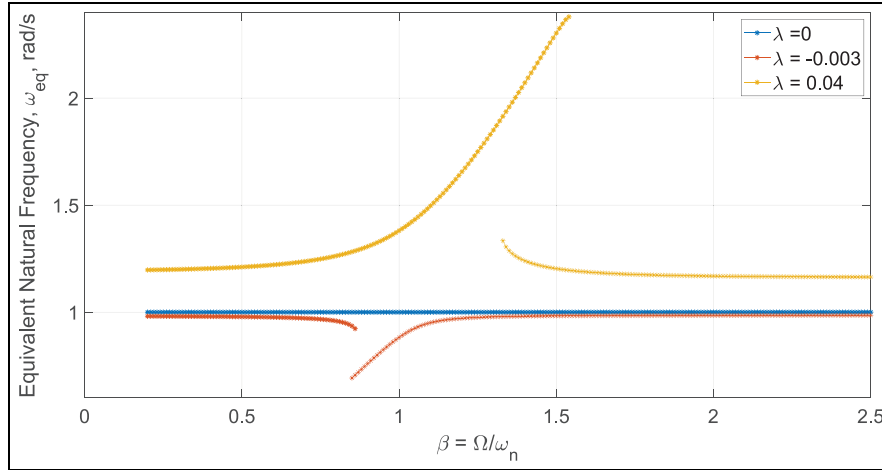
Figure 3. Equivalent Natural Frequencies for linear ($\lambda = 0$), softening ($\lambda = -0.003$) and hardening ($\lambda = 0.04$) Duffing oscillators subjected to combined harmonic and random excitation ($\lambda = -0.32$).

generation of Figure 2 the proposed equivalent linearization method takes approximately 1.8 s to obtain results for all harmonic excitation frequencies examined. Performing time integration, with 30 Monte Carlo realizations at each of the 120 excitation frequencies considered, required over 10,000 s. Therefore, the proposed method provides a reduction in computational time of four orders of magnitude in the examples above. It is acknowledged that it may be possible to improve time integration speed through use of a faster integration algorithm, such as Newmark Beta,[43] or through more optimal selection of analysis parameters such as the time step and duration. However, it is clear that the proposed method is significantly more computationally efficient.

Figure 3 shows how the linearized natural frequencies, ω_{eq}, of the systems examined above change with harmonic excitation frequency. Equivalent linear frequency represents the frequency of the equivalent linear oscillator that is used to approximate the nonlinear system, and can be calculated using the mass and linearized stiffness as:

$$\omega_{eq} = \sqrt{\frac{K_{eq}}{M}} \qquad (41)$$

The equivalent linear frequency of a linear oscillator ($\lambda = 0$) is also shown. It can be appreciated that, as expected, the equivalent natural frequency of the linear system stays constant at the natural frequency (i.e. $\omega_n = 1 \ rad/s$), while the equivalent frequencies of the softening and hardening oscillators are less than or greater than ω_n respectively. The impact of the random excitation on linearized natural frequency is evident in the frequency range away from the resonant peak, particularly for the system with hardening nonlinearity, which behaves like an oscillator with $\omega_n \approx 1.2 \ rad/s$ in this excitation frequency range. Similarly, an equivalent damping value could be

extracted for a dissipative system, although this is not relevant for the non-dissipative Duffing oscillator considered here. The ability to extract this type of information offers the possibility of more physical insight into system behavior and is the primary advantage of the EL-TEE approach over the alternative Spanos Method discussed in the next section.

Application of the Spanos method to the Duffing oscillator

This section applies the Spanos et al. Method proposed in Spanos et al.[11] and Kong and Spanos[39] for the same scenarios examined in Section 3.3. For a SDOF system with zero-mean excitation, and assuming the random excitation component is white noise, the coupled equations of the Spanos Method can be written as:

$$-\Omega^2 M v_c + \Omega C v_s + K v_c + \frac{2}{T}\int_0^T E[f_{nl}]\cos\Omega t dt - p_c = 0$$
$$(42a)$$

$$-\Omega^2 M v_s - \Omega C v_c + K v_s + \frac{2}{T}\int_0^T E[f_{nl}]\sin\Omega t dt - p_s = 0$$
$$(42b)$$

$$E[v_r^2] = \frac{\pi S_0}{2\zeta\omega_n M(K + K^*)} \qquad (42c)$$

$$K^* = \int_0^T E\left[\frac{\partial(f_{nl} - E[f_{nl}])}{\partial v_r}\right] dt \qquad (42d)$$

where harmonic excitation and displacement is written as a sum of sine and cosine terms such that:
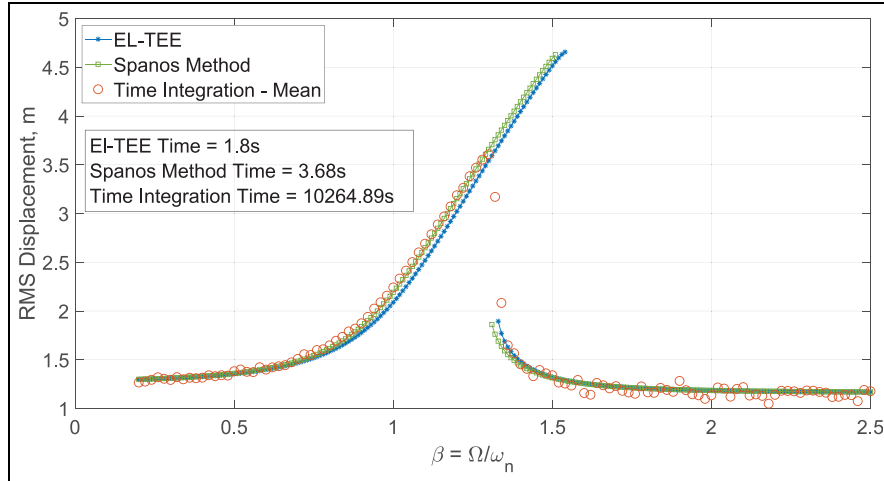
Figure 4. Comparison of the response of Duffing oscillator with hardening nonlinearity ($\lambda = 0.04$) to combined harmonic and random excitation ($\alpha = 0.32$) calculated using time integration, the proposed EL-TEE method and the Spanos Method.

$$p_h = p_c \cos \Omega t + p_s \sin \Omega t \tag{43}$$

$$v_h = v_c \cos \Omega t + v_s \sin \Omega t \tag{44}$$

Analytical solutions for the integrals in equation (41a and b) and for K^* are derived in Appendix B:

$$\frac{2}{T} \int_0^T E[f_{nl}] \cos \Omega t \, dt = \lambda \left(\frac{3}{4} v_c^3 + \frac{3}{4} v_c v_s^2 + 3E[v_r^2] v_c \right) \tag{45}$$

$$\frac{1}{T} \int_0^T E[f_{nl}] \cos \Omega t \, dt = \lambda \left(\frac{3}{4} v_s^3 + \frac{3}{4} v_c^2 v_s + 3E[v_r^2] v_s \right) \tag{46}$$

$$K^* = 3\lambda \left(\frac{v_c^2 + v_s^2}{2} + E[v_r^2] \right) \tag{47}$$

Thus, by combining equation (42) and equations (45)–(47), for a SDOF Duffing oscillator subjected to combined harmonic and white noise random excitation, the coupled equations for Spanos Method can be written as:

$$-\Omega^2 M v_c + \Omega C v_s + K v_c \\ + \lambda \left(\frac{3}{4} v_c^3 + \frac{3}{4} v_c v_s^2 + 3v_c E[v_r^2] \right) - f_c = 0 \tag{48a}$$

$$-\Omega^2 M v_s - \Omega C v_c + K v_s \\ + \lambda \left(\frac{3}{4} v_s^3 + \frac{3}{4} v_c^2 v_s + 3v_s E[v_r^2] \right) - f_s = 0 \tag{48b}$$

$$E[v_r^2] = \frac{\pi S_0}{2\zeta \omega_n M(K + K^*)} \tag{48c}$$

$$K^* = 3\lambda \left(\frac{v_c^2 + v_s^2}{2} + E[v_r^2] \right) \tag{48d}$$

Comparing equations (34) and (48), it can be seen that, unlike the K^e term in equation (34c), the K^* term in equation (48d) does not represent the complete nonlinear stiffness; the terms derived from the integrals in equation (42 a and b) also contribute to capturing the effect of the nonlinearity. This can be easily appreciated by noting that for the case of purely harmonic excitation K^* does not impact the harmonic response in equation (48a and b), but still returns a (meaningless) value of $\frac{3\lambda(v_c^2 + v_s^2)}{2}$.

Figure 4 and Supplemental Figure 2 show the results obtained for a Duffing oscillator analyzed via the Spanos Method. The system examined are the same as in Figure 2 and Supplemental Figure 1. As before, both systems are subjected to combined unit amplitude harmonic excitation and white noise excitation with constant spectral density of $S_0 = 0.05 \, \text{N}^2/$(rad/s), or $\alpha = 0.32$, and results from the Spanos approach (squares) are compared to the EL-TEE results and benchmark Monte Carlo Time Integration simulations.

For both the hardening and softening case these RMS values obtained from the Spanos approach are similar to the mean values obtained from the Monte Carlo time integration. Broadly, the results are also very similar to those obtained using EL-TEE in Figure 2. However, some minor differences are worth highlighting. Firstly, for the softening nonlinearity (Supplemental Figure 2), the Spanos approach returns converged solutions in the upper branch for
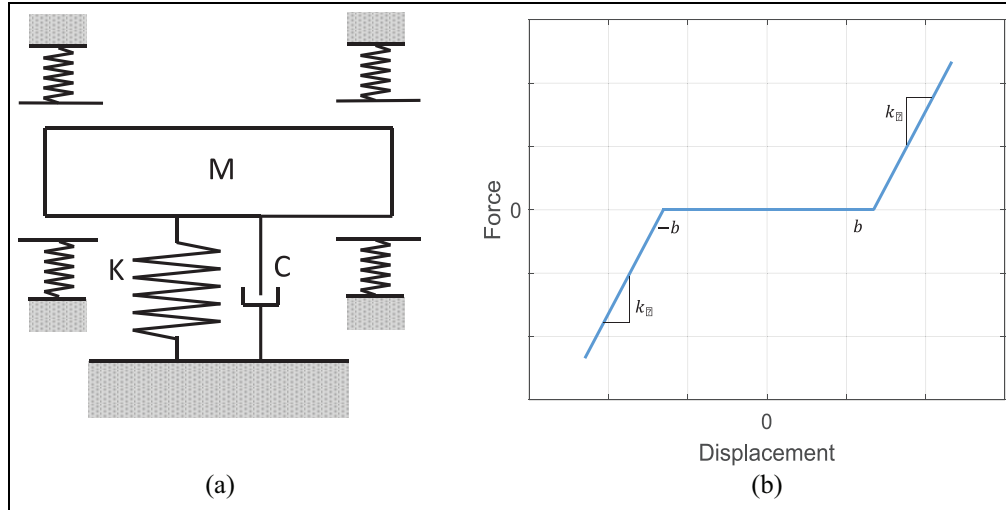
Figure 5. (a) Schematic of the system under examination and (b) the nonlinearity of the system.

harmonic excitation frequencies in the range 0.7–0.8 rad/s that are not obtained with the proposed EL-TEE approach. Secondly, comparing the hardening nonlinearity results in Figure 4, the Spanos approach appears to give a slightly better approximation of the mean Monte Carlo Time Integration response in the rising branch for harmonic excitation frequencies in the range 0.8–1.3 rad/s. This increased accuracy can be attributed to the extra degree of flexibility resulting from the separation of the harmonic and random linearization coefficients.

The computation times are approximately twice as slow for the Spanos Method (1.27 s compared to 2.67 s for the softening case and 1.8 s compared to 3.68 s for the hardening case), illustrating the slight trade-off between accuracy and complexity between the two approaches. However, the difference is small in absolute terms and computation times are still approximately four orders magnitude faster than the Monte Carlo time integration employed. Overall, it can be concluded that while the Spanos Method may be slightly more accurate in some cases, the loss in accuracy associated with using the EL-TEE approach proposed here is small. Given that performance is shown to be comparable to the Spanos approach,

and it may be beneficial to obtain physically meaningful linearization matrices, the performance of the EL-TEE method for more advanced examples is explored in the following sections.

Application to an oscillator with discontinuous nonlinearity

To demonstrate the versatility of the proposed EL-TEE approach, the method is also applied to a single degree of freedom oscillator with a pair of flexible end-stops with symmetric clearance which restrict the displacement of the mass, as illustrated in Figure 5(a). This gives the discontinuous nonlinear restoring force shown in Figure 5(b).

This piecewise nonlinearity is described by the equations:

$$
\begin{aligned}
f_{nl} &= k_s(v + b) && v < -b \\
f_{nl} &= 0 && -b < v < b \\
f_{nl} &= k_s(v - b) && v > b
\end{aligned}
\tag{49}
$$

where k_s is the nonlinear contact stiffness and b is the clearance between the end-stops. It is possible to derive a piecewise analytical solution to the integral $\int_0^T E[f_{nl}v]dt$ and a solution for $\int_0^T E[v^2]dt$. These allow an analytical expression for the equivalent stiffness matrix to be obtained, as derived in Appendix C:

$$
K^e = \frac{2k_s\left(\frac{V_h^2(2\Omega t_2 - \sin(2\Omega t_2) - 2\Omega t_1 + \sin(2\Omega t_1))}{4\Omega} + E[v_r^2](t_2 - t_1) + \frac{V_h b(\cos(\Omega t_2) - \cos(\Omega t_1))}{\Omega}\right)}{E[v_r^2]T + \frac{1}{2}V_h^2 T}
\tag{50}
$$

The nonlinear resorting force described by equation (49) is a function of both the harmonic and random response components, that is, $f_{nl}(v) = f_{nl}(v_h + v_r)$. The challenge in developing an analytical
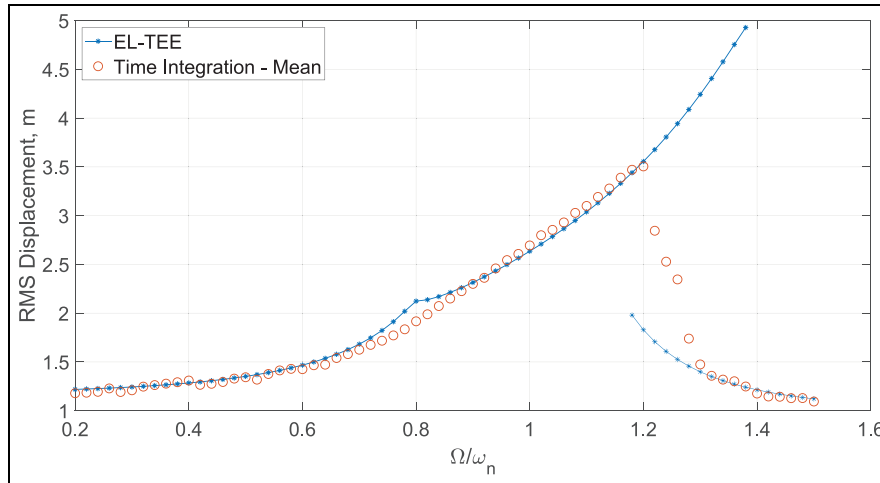
Figure 6. Comparison of the response of an oscillator with discontinuous end-stop nonlinearity to combined harmonic and random excitation ($\alpha = 0.25$) calculated using time integration and the proposed EL-TEE method.

representation of K^e for a discontinuous nonlinearity is defining when $v > b$ given the presence of a random response component. In other words, given that v is partly random, it is impossible to say which of the three piecewise equations in equation (49) is applicable at any instant. In order to overcome this issue, it is assumed that the nonlinear restoring force can be approximated as function of the harmonic response only, that is, $f_{nl}(v) \approx f_{nl}(v_h)$. This is a limitation, but is deemed a reasonable approximation as v_h is the ensemble average of v. This assumption allows the analytical solution for K^e presented in equation (50) to be developed, where t_1 and t_2 are the times in a harmonic response cycle where $v_h = b$.

As before, the oscillator examined is assigned unit mass and stiffness and 5% damping. The nonlinear parameters are chosen to be $k_s = 2$ and $b = 3$. The oscillator is subjected to combined excitation with unit harmonic amplitude and $S_0 = 0.03$, that is, $\alpha = 0.25$.

Figure 6 shows the change in the RMS displacement response with excitation frequency for this example system. Results from the proposed EL-TEE method are compared to the mean value across 30 Monte Carlo time integration realizations. Again, there is generally a good match between the two methods, though differences are apparent in several places. Firstly, as with the Duffing oscillator in the previous section, the equivalent linearization approach returns two solution branches, while the time integration results show the jump between branches occurring over a range of frequencies, illustrated by the average values across the realizations lying between the two branches. Furthermore, there are some differences between results when excitation frequency is approximately equal to 0.8 rad/s. These arise from the assumption, discussed above, that $f_{nl}(v) \approx f_{nl}(v_h)$. In this region of excitation frequencies the harmonic response amplitude is slightly less than b, meaning $f_{nl}(v_h) = 0$. However, the additional random response component means that

in reality there is some nonlinear behavior. This is observed in time integration, but is not captured by equation (50), leading to the difference in predicted response between the two approaches. The assumption appears to be reasonably valid across the remaining excitation frequencies examined.

Application to a 3 DOF oscillator & comparison with experimental results

Finally, the proposed EL-TEE approach is also applied to an experimentally tested multi-degree-of-freedom nonlinear oscillator. The experimental system, shown in Figure 7, consists of a cantilever beam clamped at one end, with magnetic constraints at the free end creating a nonlinear system. An electromagnetic shaker is used to apply load to the system, while an accelerometer is used to measure the response.

Impulse response tests were carried out with the magnetic constraint removed to obtain the natural frequencies and damping ratios of the beam. Details of the estimated parameters are provided in Supplemental Table 1.

The relationship between displacement and force was examined to quantify the nonlinearity created by the magnetic constraint. This was done by measuring both the beam acceleration, using an additional accelerometer, and magnetic force, using force sensors, at the constraint points. This is shown in Supplemental Figure 3. The measured acceleration was integrated twice to evaluate displacement, allowing the force-displacement relationship to be plotted. As shown in Figure 8, a cubic polynomial, $f = c_1 x + c_2 x^2 + c_3 x^3$, was fitted to the force-displacement relationship to quantify the nonlinearity. The coefficients obtained from this fitting process are also shown.

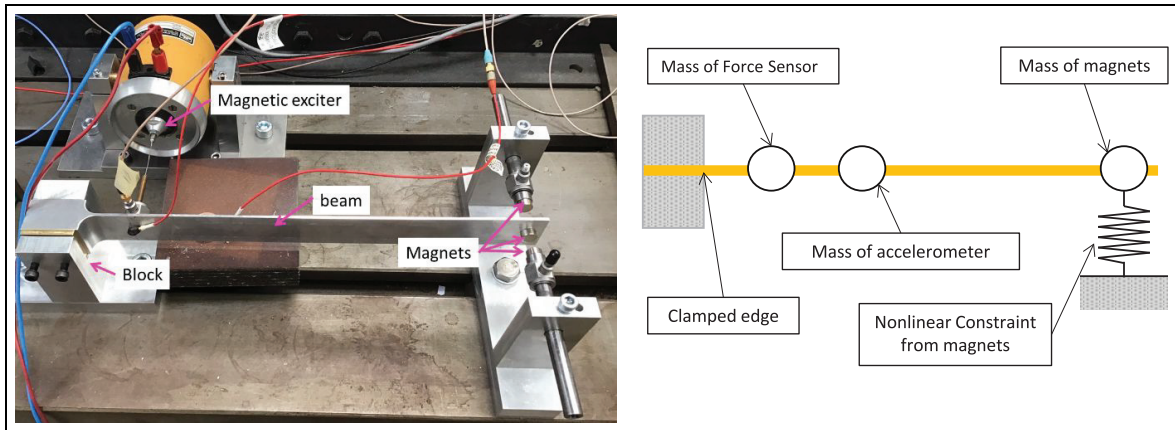Once the system is adequately characterized, the proposed equivalent linearization approach can be

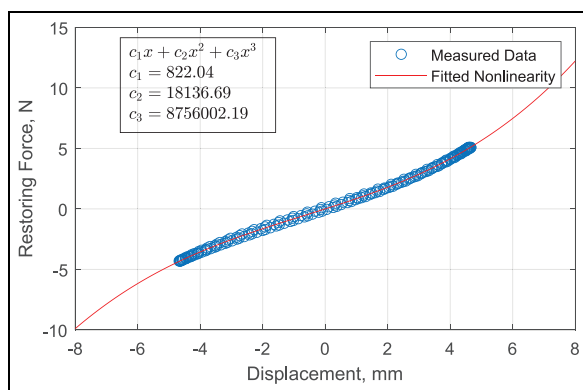**Figure 7.** Photograph and schematic of experimental setup.

Figure 8. Nonlinearity of the experimental system showing fitted polynomial and coefficients.

applied by modeling the oscillator as a three degree of freedom system, as illustrated in Figure 7. An analytical expression for the equivalent linear stiffness matrix for such a system with a localized polynomial nonlinearity at degree of freedom 3, subject to combined harmonic and random excitation, is derived in Appendix D.

A first set of experiments were performed by subjecting the system to purely harmonic excitation of amplitude 1, 2, and 5 N at frequencies ranging from 20 Hz to 50 Hz, exciting the first mode of the system. The experiments were performed for 50 harmonic loading cycles for each harmonic excitation frequency, with a sampling rate of 2 kHz. Figure 9 compares the RMS acceleration response from these experiments with the corresponding value calculated using the proposed EL-TEE approach. The proposed method captures the general key trends well, including the nonlinear jump behavior observed for the 5 N load amplitude case. However, there are also some differences between the experimental and analytical results; in particular the peak values are slightly different. These differences are most likely due to inaccuracies in the characterization of the system and do not represent a problem with the proposed method.

A second set of experiments was performed by applying combined harmonic and random excitation. The frequency of the harmonic excitation ranged between 20Hz and 50Hz with an amplitude of 5N. Zero mean white noise random excitations with constant spectral densities, S_0, equal to 2×10^{-5} N^{2}s and 1×10^{-4} N^{2}s, corresponding to $\alpha = 0.02$ and $\alpha = 0.04$ respectively, were applied. Figure 10 compares the RMS acceleration response at the measurement position obtained experimentally and calculated numerically for these cases. A similar plot for the case of purely harmonic excitation ($\alpha = 0$) is also shown for comparison. Slight differences between the numerical and experimental results can be seen in the peak value of RMS response. As before, these can be attributed to inaccuracies in the characterization of the system. However, the main features observed experimentally are reliably predicted using the EL-TEE method. Additional random excitation leads to increased RMS response, with this increase being more noticeable away from the resonance peak. This trend is noted for both the experimental and numerical results. Furthermore, for both the experimental and analytical cases the strength of the random loading component appears to have no impact on the frequency where the response "jumps" from high to low. This may be due to the experimental limitations of the current test rig where larger values for α were not possible.

Conclusion

A new method has been developed to calculate the response of nonlinear oscillators to combined random and harmonic excitation. The method is based on applying equivalent linearization across the ensemble of random responses and averaging over a single harmonic loading period, and is referred to as an Equivalent Linearization Time-and-Ensemble Expectation approach (EL-TEE). The performance of the proposed EL-TEE approach is examined for three nonlinear systems, demonstrating its wide applicability. Firstly, a single
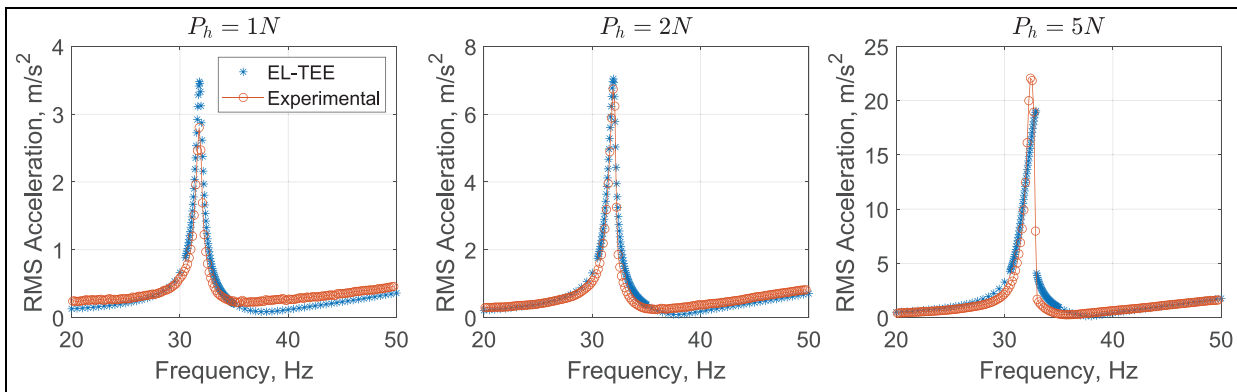
Figure 9. RMS acceleration response obtained experimentally and calculated using the proposed Time-and-Ensemble Expectation Equivalent Linearization (EL-TEE) approach for three different levels of harmonic excitation.
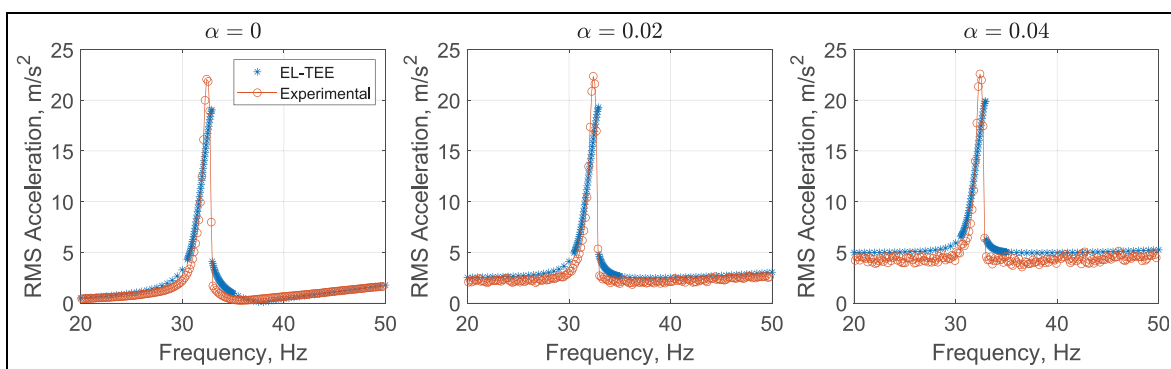

Figure 10. RMS acceleration response obtained experimentally and calculated using the proposed Time-and-Ensemble Expectation Equivalent Linearization (EL-TEE) approach for the combined random and harmonic excitation quantified by α.

degree of freedom Duffing oscillator is assessed, where the method is shown to be capable of reproducing the results of Monte Carlo Time Integration with several orders of magnitude reduction in computational cost. It is also demonstrated that performance is comparable to an alternative analysis approach recently proposed by Spanos et al.[11,39] Secondly, a single degree of freedom system with end-stops providing a discontinuous nonlinearity is examined, with the proposed approach again shown to compare well with Monte Carlo time integration. Finally, the method is applied to a multi degree of freedom cantilever beam with a localized smooth nonlinearity at the tip of the beam, for which experimental results were obtained from a laboratory test rig. Results from the equivalent linearization matched the key features of the experimental results well. The primary benefits of the proposed EL-TEE approach compared to others in the literature are the computational speed, ability to return physically meaningful linearization matrices and the adaptability to various nonlinearities and multi degree of freedom systems.

ORCID iD

John Hickey https://orcid.org/0000-0002-1727-3684

Supplemental material

Supplemental material for this article is available online.

References

1. Ellermann K. On the determination of nonlinear response distributions for oscillators with combined harmonic and random excitation. *Nonlinear Dyn* 2005; 42: 305–318.
2. Megerle B, Stephen Rice T, McBean I, et al. Numerical and experimental investigation of the aerodynamic excitation of a model low-pressure steam turbine stage operating under low volume flow. *J Eng Gas Turbine Power* 2013; 135: 012602.
3. Hawes DH and Langley RS. Numerical methods for calculating the response of a deterministic and stochastically excited duffing oscillator. *Proc IMechE, Part C: J Mechanical Engineering Science* 2016; 230: 888–899.
4. Mickens RE. Comments on the method of harmonic balance. *J Sound Vib* 1984; 94: 456–460.
5. Roberts JB and Spanos PD. *Random vibration and statistical linearization*. Courier Corporation, Mineola, New York, 2003.
6. Elishakoff I and Crandall SH. Sixty years of stochastic linearization technique. *Meccanica* 2017; 52: 299–305.
7. Hawes D. *Nonlinear stochastic vibration analysis for energy harvesting and other applications*. Thesis, Department of Engineering, University of Cambridge, UK, 2017. DOI: 10.17863/CAM.6712.
8. Iyengar RN. A nonlinear system under combined periodic and random excitation. *J Stat Phys* 1986; 44: 907–920.
9. Zhu HT and Guo SS. Periodic response of a Duffing oscillator under combined harmonic and random excitations. *J Vib Acoust* 2015; 137: 041015.
10. Haiwu R, Wei X, Guang M, et al. Response of a duffing oscillator to combined deterministic harmonic and random excitation. *J Sound Vib* 2001; 242: 362–368.
11. Spanos PD, Zhang Y and Kong F. Formulation of statistical linearization for M-D-O-F systems subject to combined periodic and stochastic excitations. *J Appl Mech* 2019; 86: 101003.
12. Anh ND and Hieu NN. The Duffing oscillator under combined periodic and random excitations. *Probab Eng Mech* 2012; 30: 27–36.
13. Anh ND, Zakovorotny VL and Hao DN. Response analysis of Van der Pol oscillator subjected to harmonic and random excitations. *Probab Eng Mech* 2014; 37: 51–59.
14. Manohar CS and Iyengar RN. Entrainment in van der Pol's oscillator in the presence of noise. *Int J Non Linear Mech* 1991; 26: 679–686.
15. Nayfeh A. Introduction to perturbation techniques. https://www.semanticscholar.org/paper/Introduction-To-Perturbation-Techniques-Nayfeh/34067a5cc5ec1fc4341240675de7bc8e63e5dea7 (1981, accessed 4 October 2021).
16. Nayfeh AH. Resolving controversies in the application of the method of multiple scales and the generalized method of averaging. *Nonlinear Dyn* 2005; 40: 61–102.
17. El-Dib YO. Modified multiple scale technique for the stability of the fractional delayed nonlinear oscillator. *Pramana J Phys* 2020; 94: 56.
18. Awrejcewicz J, Starosta R and Sypniewska-Kamińska G. *Asymptotic multiple scale method in time domain: multi-degree-of-freedom stationary and nonstationary dynamics*. Boca Raton, FL: CRC Press, 2022.
19. Du H-E, Er G-K and Iu VP. Parameter-splitting perturbation method for the improved solutions to strongly nonlinear systems. *Nonlinear Dyn* 2019; 96: 1847–1863.
20. Du H-E, Er G-K, Iu VP, et al. Constrained parameter-splitting perturbation method for the improved solutions to the nonlinear vibrations of Euler–Bernoulli cantilevers. *Nonlinear Dyn* 2023; 111: 9025–9047.
21. El-Dib Y. Stability of a strongly displacement time-delayed Duffing oscillator by the multiple-scales-homotopy perturbation method. *J Appl comput Mech* 2017; 4: 260–274.
22. El-Dib Y. Stability Analysis of a strongly displacement time-delayed Duffing oscillator using multiple scales homotopy perturbation method. *J Appl Comput Mech* 2018; 4: 260–274.
23. Anjum N and He JH. Two modifications of the homotopy perturbation method for nonlinear oscillators. *J Appl Comput Mech* 2020; 6: 1420–1425.
24. Nayfeh AH and Serhan SJ. Response statistics of nonlinear systems to combined deterministic and random excitations. *Int J Non Linear Mech* 1990; 25: 493–509.
25. Serhan SJ and Nayfeh AH. Nonlinear random coupled motions of structural elements with quadratic nonlinearities. *Nonlinear Dyn* 1991; 2: 305–316.
26. Rong H, Xu W and Fang T. Principal response of duffing oscillator to combined deterministic and narrow-band random parametric excitation. *J Sound Vib* 1998; 210: 483–515.
27. Rong H, Wang X, Xu W, et al. Resonant response of a non-linear vibro-impact system to combined deterministic harmonic and random excitations. *Int J Non Linear Mech* 2010; 45: 474–481.
28. Benedettini F, Zulli D and Vasta M. Nonlinear response of SDOF systems under combined deterministic and random excitations. *Nonlinear Dyn* 2006; 46: 375–385.
29. Haiwu R, Guang M, Xiangdong W, et al. Response statistic of strongly non-linear oscillator to combined deterministic and random excitation. *Int J Non Linear Mech* 2004; 39: 871–878.
30. Cai GO and Lin YK. Nonlinearly damped systems under simultaneous broad-band and harmonic excitations. *Nonlinear Dyn* 1994; 6: 163–177.
31. Dimentberg MF. Response of a non-linearly damped oscillator to combined periodic parametric and random external excitation. *Int J Non Linear Mech* 1976; 11: 83–87.
32. Huang ZL, Zhu WQ and Suzuki Y. Stochastic averaging of strongly non-linear oscillators under combined harmonic and white-noise excitations. *J Sound Vib* 2000; 238: 233–256.
33. Narayanan S and Kumar P. Numerical solutions of Fokker–Planck equation of nonlinear systems subjected to random and harmonic excitations. *Probab Eng Mech* 2012; 27: 35–46.
34. Wu YJ and Zhu WQ. Stochastic averaging of strongly nonlinear oscillators under combined harmonic and wide-band noise excitations. *J Vib Acoust* 2008; 130: 051004.
35. Zhu WQ and Wu YJ. First-passage time of Duffing oscillator under combined harmonic and white-noise excitations. *Nonlinear Dyn* 2003; 32: 291–305.

36. Soize C. The Fokker-Planck equation for stochastic dynamical systems and its explicit steady state solutions. *Sci World* 1994; 17: 189–217. DOI: 10.1142/2347

37. Xu W, He Q, Fang T, et al. Stochastic bifurcation in duffing system subject to harmonic excitation and in presence of random noise. *Int J Non Linear Mech* 2004; 39: 1473–1479.

38. Xie WX, Xu W and Cai L. Study of the Duffing–Rayleigh oscillator subject to harmonic and stochastic excitations by path integration. *Appl Math Comput* 2006; 172: 1212–1224.

39. Kong F and Spanos PD. Stochastic response of hysteresis system under combined periodic and stochastic excitation via the statistical linearization method. *J Appl Mech* 2021; 88: 051008. DOI: 10.1115/1.4049836

40. Vershynin R. *High-dimensional probability: an introduction with applications in data science*. Cambridge: Cambridge University Press, 2018.

41. Krack M and Gross J. *Harmonic balance for nonlinear vibration problems*. Cham, Switzerland: Springer, 2019.

42. Von Groll G and Ewins D. The harmonic balance method with arc-length continuation in rotor/stator contact problems. *J Sound Vib* 2001; 241: 223–233.

43. Newmark NM. A method of computation for structural dynamics. *J Eng Mech Div* 1959; 85: 67–94.

Appendix A

Evaluation of K^e for SDOF Duffing oscillator

For the case of a single degree of freedom system with zero-mean excitation and response and symmetric nonlinearity, the equivalent linear stiffness, given by equation (25d) reduces to:

$$K^e = \frac{\int_0^T \mathrm{E}[f_{nl}v]\mathrm{d}t}{\int_0^T \mathrm{E}[v^2]\mathrm{d}t} \tag{A.1}$$

An analytical solution requires evaluation of the integrals in both the numerator and denominator. Firstly, looking at $\int_0^T E[f_{nl}v]dt$:

$$\int_0^T \mathrm{E}[f_{nl}v]dt = \int_0^T \mathrm{E}\left[\lambda v^3 v\right]dt \tag{A.2}$$

$$\int_0^T \mathrm{E}[f_{nl}v]dt = \lambda \int_0^T \mathrm{E}\left[v^4\right]dt \tag{A.3}$$

$E[v^4]$ can be evaluated by breaking down v into harmonic and random components:

$$\int_0^T E[f_{nl}v]dt = \lambda \int_0^T E\left[(v_r + v_h)^4\right]dt \tag{A.4}$$

$$\int_0^T E[f_{nl}v]dt = \int_0^T E\left[v_h^4 + v_r^4 + 4v_h^3 v_r + 4v_h v_r^3 + 6v_h^2 v_r^2\right]dt \tag{A.5}$$

Noting that v_r is a zero mean Gaussian random variable allows the statistical moments of the random response component v_r to be written as:

$$\int_0^T E[v_r]dt = 0 \tag{A.6}$$

$$\int_0^T E\left[v_r^2\right]dt = E\left[v_r^2\right]T \tag{A.7}$$

$$\int_0^T E\left[v_r^3\right]dt = 0 \tag{A.8}$$

$$\int_0^T E\left[v_r^4\right]dt = 3\left(E\left[v_r^2\right]\right)^2 T \tag{A.9}$$

Similarly, as v_h is a sinusoid, the integrals over one period of oscillation can be written as:

$$\int_0^T E[v_h]dt = 0 \tag{A.10}$$

$$\int_0^T E\left[v_h^2\right]dt = \frac{1}{2} V_h^2 T \tag{A.11}$$

$$\int_0^T E\left[v_h^3\right]dt = 0 \tag{A.12}$$

$$\int_0^T E\left[v_h^4\right]dt = \frac{3}{8} V_h^4 T \tag{A.13}$$

Where V_h is the amplitude of v_h. Using equations (A.6)–(A.13), equation (A.5) can be simplified to:

$$\int_0^T E[f(v)v]dt = \lambda \left(\frac{3}{8} V_h^4 T + 3\left(E\left[v_r^2\right]\right)^2 T + 3V_h^2 E\left[v_r^2\right] T\right) \tag{A.14}$$

Now examining the denominator in equation (A.1), $\int_0^T E[v^2]\,dt$. Again, response can be broken down into harmonic and random components:

$$\int_0^T E[v^2]\,dt = \int_0^T E\left[(v_r + v_h)^2\right]dt \tag{A.15}$$

$$\int_0^T E[v^2]\,dt = \int_0^T E\left[v_r^2 + v_h^2 + 2v_h v_r\right]dt \tag{A.16}$$

As before, the Expectations and integrals in equations (A.6)–(A.13) can be used to simplify equation (A.16) giving:

$$\int_0^T E[v^2]\,dt = E[v_r^2]T + \frac{1}{2}V_h^2 T \tag{A.17}$$

Substituting equations (A.14) and (A.17) into equation (A.1) and simplifying leaves:

$$K^e = \frac{\lambda\left(\frac{3}{8}V_h^4 + 3\left(E[v_r^2]\right)^2 + 3V_h^2 E[v_r^2]\right)}{E[v_r^2] + \frac{1}{2}V_h^2} \tag{A.18}$$

Appendix B

Evaluation of K^* and integrals for Spanos Method applied to SDOF Duffing oscillator

Application of the Spanos Method for the Duffing oscillator in Section 2.4 requires the evaluation of the integrals in equation (42a and b) and the K^* term in equation (42d).

Firstly, examining the integral $\frac{2}{T}\int_0^T E[f_{nl}]\cos\Omega t\,dt$. The nonlinear force for a Duffing oscillator is given in equation (32). Therefore, the integral becomes:

$$\frac{2}{T}\int_0^T E[f_{nl}]\cos\Omega t\,dt = \frac{2}{T}\int_0^T E[\lambda v^3]\cos\Omega t\,dt \tag{B.1}$$

Separating the response component into random and harmonic parts, assuming a zero mean response and expanding gives:

$$\frac{2}{T}\int_0^T E[f_{nl}]\cos\Omega t\,dt = \frac{2}{T}\int_0^T E\left[\lambda\left(v_h^3 + v_r^3 + 3v_h v_r^2 + 3v_h^2 v_r\right)^3\right]\cos\Omega t\,dt \tag{B.2}$$

Evaluating the expectations for the various terms:

$$\frac{2}{T}\int_0^T E[f_{nl}]\cos\Omega t\,dt = \frac{2}{T}\lambda\int_0^T \left(v_h^3 + 3v_h E[v_r^2]\right)\cos\Omega t\,dt \tag{B.3}$$

Noting that, as per equation (43), $v_h = v_c\cos\Omega t + v_s\sin\Omega t$, and then expanding and evaluating the integrals gives:

$$\frac{2}{T}\int_0^T E[f_{nl}]\cos\Omega t\,dt = \lambda\left(\frac{3}{4}v_c^3 + \frac{3}{4}v_c v_s^2 + 3E[v_r^2]v_c\right) \tag{B.4}$$

Similarly, the integral $\frac{2}{T}\int_0^T E[f_{nl}]\sin\Omega t\,dt$ can be evaluated as:

$$\frac{1}{T}\int_0^T E[f_{nl}]\sin\Omega t\,dt = \lambda\left(\frac{3}{4}v_s^3 + \frac{3}{4}v_c^2 v_s + 3E[v_r^2]v_s\right) \tag{B.5}$$

The expression for K^* is given by equation (41d) as:

$$K^* = \int_0^T E\left[\frac{\partial(f_{nl} - E[f_{nl}])}{\partial v_r}\right]dt \tag{B.6}$$

Which for the Duffing nonlinearity becomes:

$$K^* = \int_0^T E\left[\frac{\partial(\lambda v^3 - E[\lambda v^3])}{\partial v_r}\right]dt \tag{B.7}$$

Again, noting that $v = v_r + v_c\cos\Omega t + v_s\sin\Omega t$, expanding, taking expectations and derivatives leaves:

$$K^* = \int_0^T \lambda\left(3E[v_r^2] + 3v_c^2\cos^2\Omega t + 3v_s^2\sin^2\Omega t + 6v_s v_c\cos\Omega t\sin\Omega t\right)dt \tag{B.8}$$

Evaluating the integrals leaves:

$$K^* = 3\lambda\left(\frac{v_c^2 + v_s^2}{2} + E[v_r^2]\right) \tag{B.9}$$

Appendix C

Evaluation of K^e for end-stop nonlinearity

This piecewise nonlinearity is described by equation (49):

$$
\begin{aligned}
f_{nl} &= k_s(v + b) & v < -b \\
f_{nl} &= 0 & -b < v < b \\
f_{nl} &= k_s(v - b) & v > b
\end{aligned}
\tag{C.1}
$$

The Equivalent Stiffness term for a single degree of freedom system is given by equation (A.1). To evaluate this, it is necessary to evaluate $\int_0^T E[f_{nl}v]dt$ in a piecewise manner:

$$\int_0^T E[f_{nl}v]dt = \int_{t_1}^{t_2} E[k_s(v + b)v]dt + \int_{t_3}^{t_4} E[k_s(v - b)v]dt \tag{C.2}$$

Looking at the first piecewise section, which occurs between times t_1 and t_2:

$$\int_{t_1}^{t_2} E[f_{nl}v]dt = \int_{t_1}^{t_2} E[k_s(v+b)v]dt \tag{C.3}$$

This can be rearranged as:

$$\int_{t_1}^{t_2} E[f_{nl}v]dt = k_s \int_{t_1}^{t_2} E[v^2 + bv]dt \tag{C.4}$$

As per equation (14), v can be divided into harmonic and random components. It is assumed the mean displacement, $\bar{v}$ is 0. Applying this to equation (B.4), expanding and taking expectations gives:

$$\int_{t_1}^{t_2} E[f_{nl}v]dt = k_s \left(\int_{t_1}^{t_2} v_h^2 dt + \int_{t_1}^{t_2} E[v_r^2]dt + b\int_{t_1}^{t_2} v_h dt \right) \tag{C.5}$$

Evaluating these integrals:

$$\int_{t_1}^{t_2} E[f_{nl}v]dt = k_s \left(\frac{V_h^2(2\Omega t_2 - \sin(2\Omega t_2) - 2\Omega t_1 + \sin(2\Omega t_1))}{4\Omega} + E[v_r^2](t_2 - t_1) + \frac{V_h b(\cos(\Omega t_2) - \cos(\Omega t_1))}{\Omega} \right) \tag{C.6}$$

where V_h is the amplitude and Ω is the frequency of the harmonic excitation. As discussed in the body of the paper, the values of t_1 and t_2 can be approximated by assuming that they follow the ensemble average of v, which is the harmonic response component v_h. This is a limitation, but is deemed a reasonable approximation based on the ensemble average. Thus:

$$t_1 = \frac{1}{\Omega}\sin^{-1}\left(\frac{b}{V_h}\right) \tag{C.7}$$

$$t_2 = \frac{T}{2} - t_1 \tag{C.8}$$

Similarly, the second piecewise section can be evaluated as:

$$\int_{t_3}^{t_4} E[f_{nl}v]dt = k_s \left(\frac{V_h^2(2\Omega t_4 - \sin(2\Omega t_4) - 2\Omega t_3 + \sin(2\Omega t_3))}{4\Omega} + E[v_r^2](t_4 - t_3) - V_h b(\cos(\Omega t_4) - \cos(\Omega t_3)) \right) \tag{C.9}$$

where t_1 and t_2 can be approximated as:

$$t_3 = t_1 + \frac{T}{2} \tag{C.10}$$

$$t_4 = t_2 + \frac{T}{2} \tag{C.11}$$

Combining equations (C.6)–(C.11), it can be shown that:

$$\int_0^T E[f_{nl}v]dt = 2k_s\left(\frac{V_h^2(2\Omega t_2 - \sin(2\Omega t_2) - 2\Omega t_1 + \sin(2\Omega t_1))}{4\Omega} + E[v_r^2](t_2 - t_1) + \frac{V_h b(\cos(\Omega t_2) - \cos(\Omega t_1))}{\Omega}\right)$$

(C.12)

The expression for the denominator in the equivalent stiffness term defined in equation (A.1) is the same as for the Duffing oscillator:

$$\int_0^T E[v^2]dt = \sigma_{vr}^2 T + \frac{1}{2}V_h^2 T$$

(C.13)

Thus:

$$K^e = \frac{2k_s\left(\frac{V_h^2(2\Omega t_2 - \sin(2\Omega t_2) - 2\Omega t_1 + \sin(2\Omega t_1))}{4\Omega} + E[v_r^2](t_2 - t_1) + \frac{V_h b(\cos(\Omega t_2) - \cos(\Omega t_1))}{\Omega}\right)}{\sigma_{vr}^2 T + \frac{1}{2}V_h^2 T}$$

(C.14)

Appendix D

Evaluation of $\hat{K}^e$ for a 3 DOF oscillator with polynomial nonlinearity

The system under consideration is a 3 DOF oscillator, excited at DOF 1 with a localized nonlinearity, described by a third order polynomial, at DOF 3. The equivalent linear stiffness matrix can be calculated from by equation (25d):

$$\hat{\mathbf{K}}^e = \left[\int_0^T E[\Phi^T\mathbf{f_{nl}y}^T]dt\right]\left[\int_0^T E[\mathbf{yy}^T]dt\right]^{-1}$$

(D.1)

where Φ is a matrix of mode shapes and $\mathbf{y}$ is a vector of displacements in modal coordinate**s**. Development of an analytical expression involves the evaluation of two integrals. Firstly, $\int_0^T E[\Phi^T\mathbf{f_{nl}y}^T]dt$ is examined. In the case under examination, the nonlinearity is localized to degree of freedom 3.

$$\mathbf{f_{nl}} = \begin{Bmatrix} 0 \\ 0 \\ f_3 \end{Bmatrix}$$

(D.2)

$$f_3 = c_2 v_3^2 + c_3 v_3^3$$

(D.3)

If two modes are considered, pre-multiplication by Φ^T to convert to modal coordinates gives:

$$\Phi^T\mathbf{f_{nl}} = \begin{bmatrix} \phi_1^1 & \phi_2^1 & \phi_3^1 \\ \phi_1^2 & \phi_2^2 & \phi_3^2 \end{bmatrix}\begin{Bmatrix} 0 \\ 0 \\ f_3 \end{Bmatrix} = \begin{Bmatrix} \phi_3^1 f_3 \\ \phi_3^2 f_3 \end{Bmatrix}$$

(D.4)

where ϕ_q^p refers to the value of qth mode shape at degree of freedom q. Thus the integral $\int_0^T E[\Phi^T\mathbf{f_{nl}y}^T]dt$ can be written as:

$$\int_0^T E[\Phi^T\mathbf{f_{nl}y}^T]dt = \int_0^T E\left[\begin{Bmatrix} \phi_3^1 f_3 \\ \phi_3^2 f_3 \end{Bmatrix}\{y_1 \quad y_2\}\right]dt = \int_0^T E\begin{bmatrix} \phi_3^1 f_3 y_1 & \phi_3^1 f_3 y_2 \\ \phi_3^2 f_3 y_1 & \phi_3^2 f_3 y_2 \end{bmatrix}dt$$

(D.5)

This means that in matrix index notation the (i, j) element of the matrix $\int_0^T E[\Phi^T\mathbf{f_{nl}y}^T]dt$ can be written as:

$$\int_0^T E[\mathbf{\Phi}^T \mathbf{f_{nl}} \mathbf{y}^T]_{i,j} dt = \int_0^T E[\phi_3^p f_3 y_q] \ dt \tag{D.6}$$

Equation (D.6) is written in modal coordinates, but in equation (D.3) f_3 is calculated in terms of natural coordinates. Displacement at degree of freedom 3 in natural coordinates is obtained as:

$$v_3 = \phi_3^1 y_1 + \phi_3^2 y_2 \tag{D.7}$$

Thus, the nonlinear restoring force is given as:

$$f_3 = c_2(\phi_3^1 y_1 + \phi_3^2 y_2)^2 + c_3(\phi_3^1 y_1 + \phi_3^2 y_2)^3 \tag{D.8}$$

This can be expanded as the summation:

$$f_3 = c_2 \sum_m \sum_n \phi_3^m y_m \phi_3^n y_n + c_3 \sum_p \sum_q \sum_s \phi_3^p y_p \phi_3^q y_q \phi_3^s y_s \tag{D.9}$$

where all summations are performed over all the modes considered. Substituting equation (D.9) into equation (D.6) gives:

$$\int_0^T E[\mathbf{\Phi}^T \mathbf{f_{nl}} \mathbf{y}^T]_{i,j} dt = \int_0^T E\left[\phi_3^i \left(c_2 \sum_m \sum_n \phi_3^m y_m \phi_3^n y_n + c_3 \sum_p \sum_q \sum_s \phi_3^p y_p \phi_3^q y_q \phi_3^s y_s\right) y_j\right] dt \tag{D.10}$$

For clarity, the summations are addressed separately in the following equations. Firstly, looking at the square part of equation (D.10):

$$\int_0^T E\left[\phi_3^i c_2 \left(\sum_m \sum_n \phi_3^m y_m \phi_3^n y_n\right) y_j\right] dt = \sum_m \sum_n c_2 \phi_3^i \phi_3^m \phi_3^n \int_0^T E[y_n y_m y_j] dt \tag{D.11}$$

By breaking down y into harmonic and random components, expanding, evaluating the various expectations and assuming the mean displacement is zero, it can be shown that this term reduces to zero.

Thus equation (D.10) reduces to just the summation corresponding to the cubic term:

$$\int_0^T E[\mathbf{\Phi}^T \mathbf{f_{nl}} \mathbf{y}^T]_{i,j} dt = \int_0^T E\left[\phi_3^i \left(c_3 \sum_p \sum_q \sum_s \phi_3^p y_p \phi_3^q y_q \phi_3^s y_s\right) y_j\right] dt \tag{D.12}$$

$$\int_0^T E[\mathbf{\Phi}^T \mathbf{f_{nl}} \mathbf{y}^T]_{i,j} dt = \sum_p \sum_q \sum_s c_3 \phi_3^i \phi_3^p \phi_3^q \phi_3^s \int_0^T E[y_p y_q y_s y_j] dt \tag{D.13}$$

Again, y can be broken down into harmonic and random components and expanded. The expectations and integrals given in equations (D.14)–(D.18) allow further simplification:

$$E[y_r] = 0 \tag{D.14}$$

$$\int_0^T E[y_h] dt = 0 \tag{D.15}$$

$$\int_0^T y_{h,p} y_{h,q} y_{h,s} y_{h,j} dt = \frac{Y_p Y_q Y_s Y_j T}{8} \left(\cos(\theta_p + \theta_q - \theta_s - \theta_j) + 2\cos(\theta_p - \theta_q)\cos(\theta_s - \theta_j) \right) \tag{D.16}$$

Where Y_p is the amplitude and θ_p is the phase angle of $y_{h,p}$, and likewise for the other subscripts.

$$E[y_{r,q} y_{r,j}] \int_0^T y_{h,r} y_{h,s} dt = E[y_{r,q} y_{r,j}] \frac{Y_r Y_j T}{2} \cos(\theta_r - \theta_j) \tag{D.17}$$

$$E[y_{r,q} y_{r,r} y_{r,s} y_{r,j}] = E[y_{r,q} y_{r,r}] E[y_{r,s} y_{r,j}] + E[y_{r,q} y_{r,s}] E[y_{r,r} y_{r,j}] + E[y_{r,q} y_{r,j}] E[y_{r,s} y_{r,r}] \tag{D.18}$$

Application of equations (D.14)–(D.18) leads to the analytical solution to the integral $\int_0^T E[y_q y_r y_s y_j] dt$:

$$\int_0^T E[y_q y_r y_s y_j] dt = \frac{Y_q Y_r Y_s Y_j T}{8} \left(\cos(\theta_q + \theta_r - \theta_s - \theta_j) + 2\cos(\theta_q - \theta_r)\cos(\theta_s - \theta_j) \right) + E[y_{r,q} y_{r,r}] E[y_{r,s} y_{r,j}] +$$

$$E[y_{r,q} y_{r,s}] E[y_{r,r} y_{r,j}] + E[y_{r,q} y_{r,j}] E[y_{r,s} y_{r,r}] + E[y_{r,p} y_{r,q}] \frac{Y_s Y_j T}{2} \cos(\theta_s - \theta_j) +$$

$$E[y_{r,p} y_{r,s}] \frac{Y_q Y_j T}{2} \cos(\theta_q - \theta_j) + E[y_{r,p} y_{r,j}] \frac{Y_s Y_q T}{2} \cos(\theta_s - \theta_q) + E[y_{r,q} y_{r,s}] \frac{Y_p Y_j T}{2} \cos(\theta_p - \theta_j)$$

$$+ E[y_{r,q} y_{r,j}] \frac{Y_p Y_s T}{2} \cos(\theta_p - \theta_s) + E[y_{r,q} y_{r,j}] \frac{Y_p Y_s T}{2} \cos(\theta_p - \theta_s) + E[y_{r,j} y_{r,s}] \frac{Y_p Y_q T}{2} \cos(\theta_p - \theta_q) \tag{D.19}$$

From equation (D.19) an analytical solution for the (i,j) element of $\int_0^T E[\mathbf{\Phi}^\mathbf{T} \mathbf{f_{nl}} \mathbf{y}^\mathbf{T}] dt$ can be obtained:

$$\int_0^T E[\mathbf{\Phi}^\mathbf{T} \mathbf{f_{nl}} \mathbf{y}^\mathbf{T}]_{i,j} dt = \sum_{p=1}^N \sum_{s=1}^N \sum_{q=1}^N c_3 \phi_3^i \phi_3^q \phi_3^r \phi_3^s \int_0^T E[y_p y_q y_s y_j] dt \tag{D.20}$$

This is the first term in required for the calculation of the equivalent stiffness matrix in equation (D.1). The second term required, $\int_0^T E[\mathbf{y}\mathbf{y}^\mathbf{T}] dt$, is more straightforward to calculate. Breaking down the modal response into random and harmonic components, expanding and taking expectations allows the (i,j) element of $\int_0^T E[\mathbf{y}\mathbf{y}^\mathbf{T}] dt$ can be written as:

$$\int_0^T E[\mathbf{y}\mathbf{y}^\mathbf{T}]_{i,j} dt = \int_0^T y_{h,i} y_{h,j} dt + \int_0^T E[y_{r,i} y_{r,j}] dt \tag{D.21}$$

Evaluating these integrals gives:

$$\int_0^T E[\mathbf{y}\mathbf{y}^\mathbf{T}]_{i,j} dt = \frac{Y_{h,i} Y_{h,j} T}{2} \cos(\theta_i - \theta_j) + E[y_{r,i} y_{r,j}] T \tag{D.22}$$

Using equations (D.20) and (D.22) for the numerator and denominator respectively, the Equivalent Linear stiffness matrix for the system under examination to be calculated via equation (D.1).